INFN Istituto Nazionale di Fisica Nucleare
LABORATORI NAZIONALI DI FRASCATI
SIS – Pubblicazioni

**LNF–06/ 29 (IR)**
**7 Novembre 2006**

# FLUORESCENCE ANALYSIS BY SPECTROSCOPY TRANSMISSION AND ELECTRON STREAK CAMERA (FASTEST-CAM)

***A proposal for detecting time-synchronized ultra-fast light phenomena***

Andrea La Monaca[1], Giorgio Cappuccio[1,2], Roberto De Masi[3], Andrea Maria Di Lellis[4], Paolo Di Muro[5], Roberto Favilla[6], Fabrizio Fiori[7], Pasqualino Gaudio[8], Michele Maffia[3], Paolo Mariani[9], Alberto Mazzini[10], Ivan Micetich[5], Domenico Nanni[11], Maria Richetta[10], Franco Rustichelli[7], Benedetto Salvato[5], Francesco Spinozzi[9]

[1]*Laboratori Nazionali di Frascati dell'INFN, Frascati, Italy*

[2]*Istituto di Struttura dei Materiali Nanometrici del CNR, Roma, Italy*

[3]*Dipartimento di Scienze e Tecnologie Biologiche ed Ambientali dell'Università di Lecce, Lecce, Italy*

[4]*AMDL-P.M.I. Settore Spaziale, Roma, Italy*

[5]*Dipartimento di Biologia dell'Università di Padova, Padova, Italy*

[6]*Dipartimento di Biochimica e Biologia Molecolare dell'Università di Parma, Parma, Italy*

[7]*Sezione di Scienze Fisiche del Dipartimento di Medicina dell'Università Politecnica delle Marche, Ancona, Italy*

[8]*Dipartimento di Ingegneria dell'Impresa dell'Università di Tor Vergata, Roma, Italy*

[9]*Sezione di Scienze Biologiche del Dipartimento di Scienze Applicate ai Sistemi Complessi dell'Università Politecnica delle Marche, Ancona, Italy*

[10]*Dipartimento di Fisica dell'Università di Parma, Parma, Italy*

[11]*Osservatorio Astronomico di Roma del INAF, Roma, Italy*

## Abstract

Aim of FASTEST-CAM experiment is to develop and build at Frascati a new instrumentation for detecting ultra-fast light phenomena in a large frequency spectrum extended from X-rays to infrared. The apparatus is based on a customized 'streak camera', realized at reasonable cost and using an architecture open to future applications (e. g. Adrontherapy). The instrumentation will be applied: 1) to carry out fluorescence measurements of complex systems with very high time and space resolutions, using a monochromatic UV beam of wavelength 280 nm of synchrotron radiation of DAΦNE; 2) for diagnosing movement instabilities of the electron bunches and time-space emission fluctuations of the light pulses delivered by the machine or by the new ultra fast light sources, FEL, in development in LNF.

*PACS*: 07.50.e; 07.85.Qe; 41.60.Cr; 52.70.-m; 78.47.+p; 87.80-y

*Keywords*: Streak-camera; Fluorescence; Time synchronization; Bunch instability.

### 1.1 Fluorescence experiment

The experimental fluorescence setup, represented in fig. 1, consist of an UV monochromatic source (280 nm light beam from DAΦNE synchrotron radiation); a target of haemocyanin – Hc ($O_2$ transport protein in some species of invertebrates); a detecting system composed of a holographic grating to disperse in wave length the fluorescence spectrum emitted by the Hc; a 'streak camera', synchronized with the machine 'bunches', to collect the signal from the grating; the integrated electronic equipment to acquire, control, elaborate and transfer the data. This last stage is highly integrated and of large calculus power, imported and adapted from spatial physics.

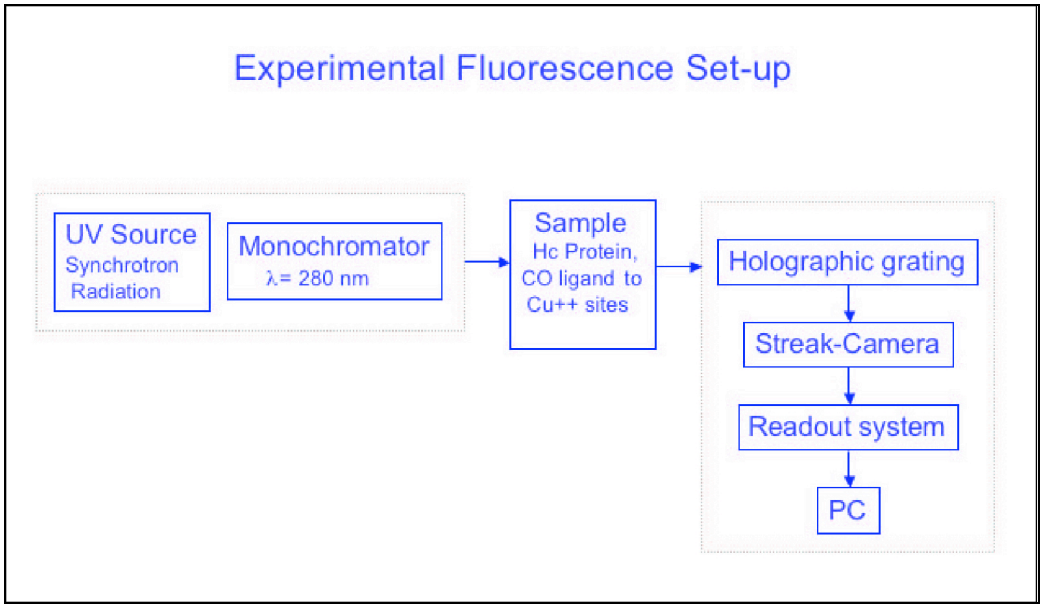


Fig. 1: Experimental fluorescence set-up.

The sample of haemocyanin (Hc) (respiratory Cu-containing protein, present in the hemolymph of several invertebrates as molluscs and arthropods), has been chosen because of its peculiarity consisting in binucleare active site. Two Cu+ (deoxyHc), each bound to three histidine's imidazol groups, bond molecular di-oxygen in a μ-peroxo bridge mode, giving the oxyHc form. The oxygen bonding (one molecule per active-site) is reversible, on going to oxygenated state (oxyHc), Cu+ turns valence state, being formally present as $Cu^{2+}$, while $O_2$ is consequently bond as peroxide. This active site has a large capability to accept the substitution of $O_2$ bond with other exogenous ligands, but also the isomorphic substitution of the constitutional Cu itself, with other metals of the 1° e 2° transition series. These exchanges influence the properties of fluorescence emissions of the aromatic amino-acids, tyroxine and tryptophan, present in Hc molecule. These fluorescence emissions differently respond following both 1) the ligand nature and 2) the nature and redox state of the two metal centres. In this contest, the carbon mono-oxide (CO) (that is dangerous for biological function of respiration, as it is known), represents a particular case, since its bonding in the Hc active site, causes a strong quenching of the light emission band with $\lambda_{max}$ at 340 nm, as it happens with other ligands, but also elicits a relatively intense emission band with $\lambda_{max}$ at 540 nm, never observed with other ligands. Quenching entity is inversely correlated to the emission intensity at 540 nm. Quenching from molecules in solution can be partially explained by energy transfer mechanism in which the excited molecule transfers part of its energy to the close environment and an other part is instead spent in fluorescence emission at lower energy with a lifetime $\tau$ less than natural lifetime $\tau_o$ (see fig. 2). This mechanism depends from oxygen ion concentration,

pH and peculiarity of the groups bindings Cu and from steric arrangement and orientation of aromatic residues, present around copper active site of protein. There is a direct relation between lifetime and quencher concentration. Life times and variation of life time under 20 ps have been found [1].

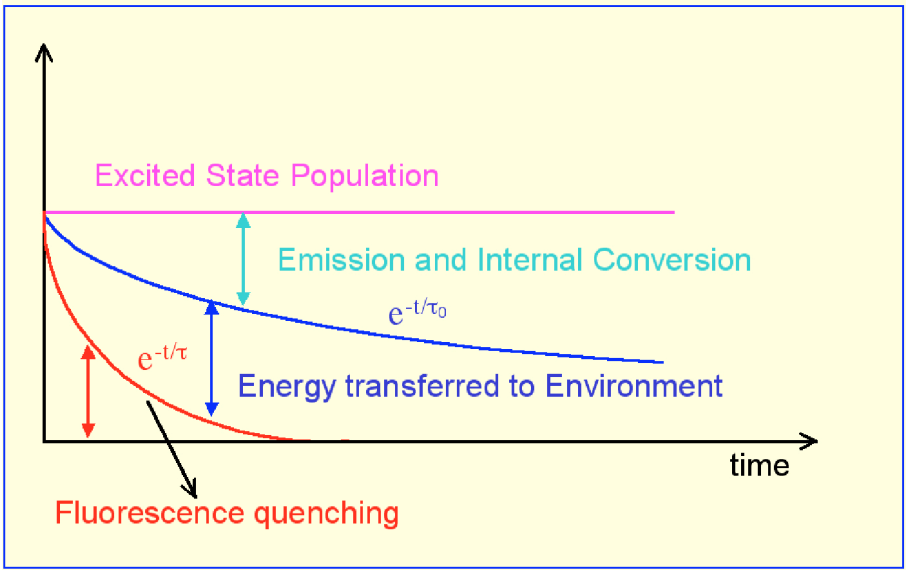


Fig.2: Return of molecules from the excited state.

The 'quenching' that is observed in Hc-deoxy is instead due to the 'heavy metal' effect of Cu+, while that is observed in Hc-oxy to the paramagnetic effect of Cu++ and of bond oxygen. In the case of the HcCO we have interesting indications that CO bondings does not occurs following a bridging mode between the two metals,as oxygen, but the bonding occurs by bridging CO molecule between the more accessible Cu+ and the H-N of indol ring of a suitably localized and oriented tryptophan. The molecular orbital that is formed after CO bonding, has got higher electronic density and lower energy, so that the fluorescence emission of the tryptophan shifts from 340 nm, simulating the quenching at this wavelength, and it is observed at 540 nm.

We will use samples of HcCO (produced from Hc and CO) incorporated in disaccharide glass with a technical process gotten ready by Padua collaboration group [2]. The lyophilized powders from HcCO solutions in disaccharide solid matrix with a ratio from 1:1 to 1:4, can also undergo strong pressures (over 15000 bars), obtaining small vitreous sheets easily handy. In the samples, so produced, it is possible to modify greatly fluorescence lifetimes and quantum efficiency, beginning from the solution values because the pressure distorts in oriented way the protein conformation, deforming the disaccharide cage, whose each one keeps a molecule of Hc CO (to note the above compression only happens in the direction of the applied force and it is not centre-symmetric). A model supposed by group of Padua collaboration, makes the consideration that emission depends from the molecular group in which CO is bound like bridge on the carbon side to more extern Cu ion, while the oxygen is bond as hydrogen bridge to H-N= of a tryptophan indolic ring. In our experiment we will measure 1) the ultra short lifetimes with the required high time resolution and 2) the emission/quenching intensity in function of the CO concentration of these samples, that, so treated, will not suffer any radiation damage relatively high intensity of synchrotron light beam, also in the case of repeated irradiations (data of Padua collaboration group). The large peculiarities of these 'bio-glasses' are so important as to open new perspectives in the developing of preparation methods of the biologic materials, adapted to technique using synchrotron radiation. This fluorescence technique, resolved at picosecond, can also give specific information on single molecule. And

this is very important for biologic systems having molecular pathologies, like in the case of membranes and DNA (specific themes of Parma collaboration group).

### 1.2 Light beam diagnostic

The visualization of the light pulses space-time fluctuations will be another interesting point to develop the camera. In fact, the developed apparatus, will be able to study, visualize and monitor the transverse motion instabilities, the electron bunches longitudinal length, the interaction with the electromagnetic field together with the space-time structure evolution of the ultra-fast light pulses delivered by the new FEL sources (SPARC, SPARX/INO), in development at LFN. Therefore the camera could be a very good system for the diagnostic of the light beam.

## 2. The Spectrometer

The first element of the spectrometer is constituted by a transmission holographic grating of 50x50x5 $mm^3$, having 1200 lines/mm with 0.008 nm of resolution at 500 nm of wavelength, mounted on a guide with a focal objective, placed behind the entrance window, that limits and focuses to infinite the light coming from the sample (see fig. 3). Behind holographic grating there is the FASTEST-CAM, which detects and acquires spectra or images.

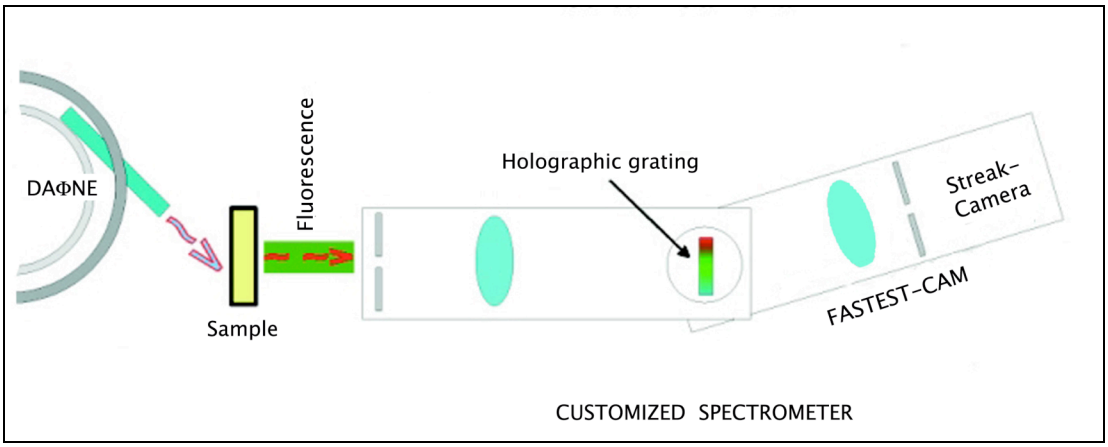


Fig 3: Spectrometer: Holographic grating and streak-camera.

### 2.1 FASTEST-CAM

FASTEST-CAM is a detector based on Streak Camera, therefore capable to measure ultra fast light phenomena and to show time or position distribution of the intensity. It can measure, in fact, either temporal variations of the incident light intensity with respect to the wavelength (time resolved spectroscopy) or temporal variations of the incident light intensity with respect to the position (time and space-resolved measurement). There is not any other instrument that can directly and so fast detect light phenomena with such a high time resolution, except for this class [3]. FASTEST-CAM operating principle is illustrated in fig. 4. Sample light passing through the holographic grating is projected onto a slit and hits a photocathode placed on the focal plane of the entry optical system. There, light pulses of different intensity, time sequence and space distribution are converted in electrons proportional, in number and kinetic energy, to the relative intensity and energy of the incident light.

The so created electrons are swept by electrodes, whose characteristic impedance is adapted to the output impedance of a radiofrequency amplifier, synchronised in time with a multiple of the bunch radiofrequency of incident synchrotron radiation of DAΦNE.

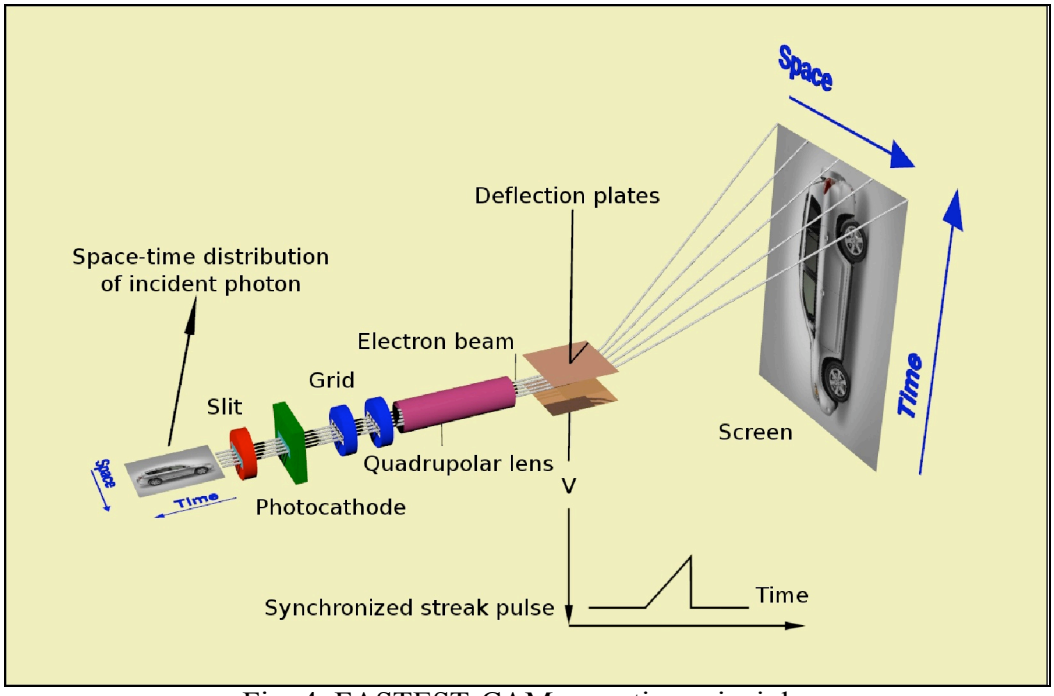


Fig. 4: FASTEST-CAM operating principle.

### 2.1.1 Time synchronization

The electronic system for time synchronization is schematized by fig. 5.

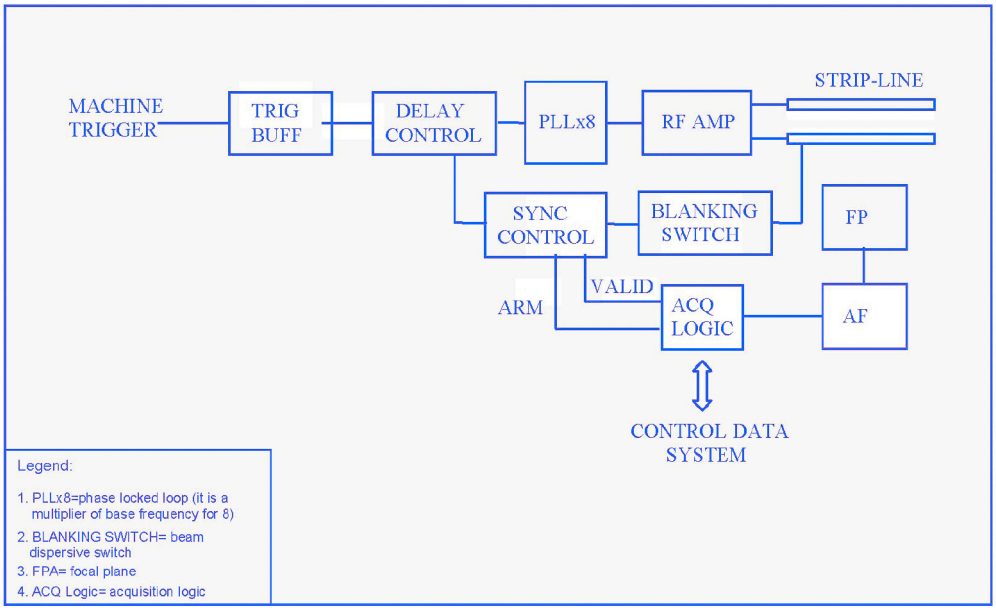


Fig. 5: Time synchronization system scheme.

In this scheme, the radiofrequency of machine, taken as reference, and that of the deflection plates, generated at more high frequency, are sent to a closed phase locked loop (PLL), which compares them in phase and shows them linked in frequency, as shown in principle in fig. 6. You see from it, since the frequency at +IN is much higher than at –IN, the output spends most of its time in the high state. The first rising edge on +IN sends the output

high and this is maintained until the first rising edge occurs on –IN. In a practical system this means that the output is driven higher, resulting in an increase in frequency at –IN.

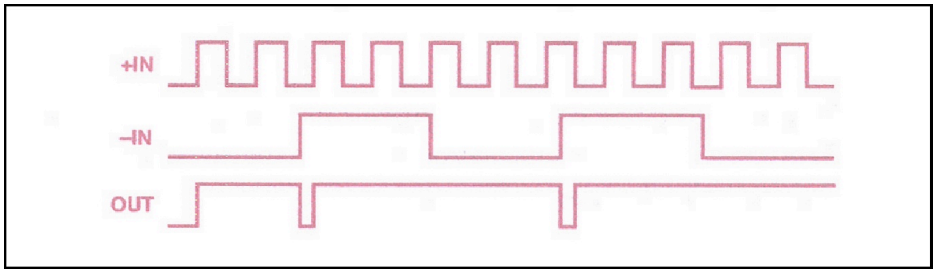


Fig. 6: PLL synchronism at fixed phase between waveforms of different frequency.

All the PLL output pulses cannot clearly be processed, since the ASIC chip read-out time takes <10 μsec. Therefore, during this time, the sequencer logic will hold the acquisition, locking the PLL out signal in order to blank the electron beams of following bunches out from the sensor until the read-out will not be ended.

### 2.1.2 Electron beam deflection

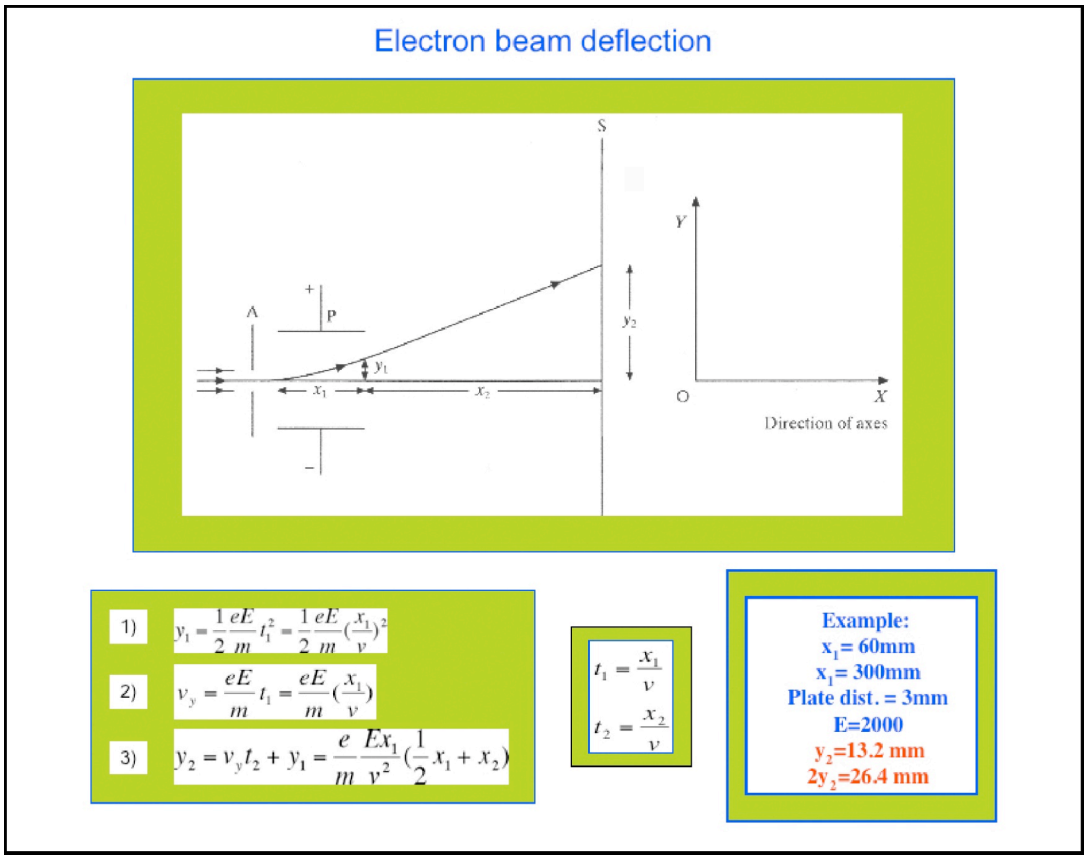


Fig. n. 7: Formulation and calculation of the electron deflection. Right bottom is reported a numeric example.

From calculation and simulation on deflection cell geometry, it has been seen, that, in our case, few volts of polarization voltage on the plates of length 3 cm and distant 3 mm between them are enough for the required temporal dispersion of the electronic beam (fig. n. 7).

Forward to the dispersion cell, the electrons go trough a second flight cell length of about 30 cm (such a region allows a magnification of space dispersion of electronic beam). Here, there is a second system of plates that allows defocusing the following fluorescence electrons, linked to the following machine bunches, in a dead zone of the detector. In this way, the radiofrequency field can operate in stable and continuous manner, while the correlation and synchronization systems of the events allow to operate and process data relative to a single trigger, without any event overlapping. Because of the used electric low voltage (due to the identify geometry) and of the plate driver that happens by direct current coupling, the plates cannot have electric tension driftage (i.e. the sweeping plates and those of blocking are separated and driven by different circuits, coupled by direct current).

### 2.1.3 Time resolution consideration

In the usual technical terminology of the streak camera the deflection voltage applied to the plates provides the 'time base'. In fact, we can see that in our previous example we have applied to the plates 20 volts/cm. This value is called 'deflection sensitivity'. Since our 'drive pulse' comes from PLL (the machine radiofrequency, ~350 MHz, multiplied per 8), and its rise time on the deflection plates is inside 1/4 of period of PLL frequency. we have (6V/170psec)=3.5 $10^{-2}$ V/psec. Therefore, our time base will be > 550 psec/cm. If we are going to consider the distance between the deflection plates and the beam detector, we will have a magnification scale of the order of 10 and the deflection velocity will also increase for the same factor. Therefore, the time base on detector will scale to about 50 psec/cm or ~250 femtosec/50μm on a MCP channel size of 50 μm.

Nevertheless, to have an estimation of the overall time resolution of streak camera apparatus it is also necessary to consider i) the dispersion effect from the photocathode space charge and ii) the dispersion time [4].

The first effect can be a severe limitation, because $10^3$ photoelectrons, for example, liberated in less than 1psec in an area of 10 $\mu m^2$, correspond to a current density of over 100 $A/cm^2$. This is sufficient to collapse a strong field close photocathode for which the chromatic time dispersion will increase, the dynamic range will reduce and the pulse output will not be longer linearly proportional to the light input.

The dispersion time is instead due 1) to the finite diameter of the optical beam, 2) to the photoelectron emission velocity spread, 3) to the transfer properties of the image (MTF). With special shrewdness these effect can be reduced to values less than seen above.

### 2.1.4 Correction for the terrestrial magnetic field

The terrestrial magnetic field can strongly interact with the electrons moving along the streak camera axis, deflecting their path. To calculate this effect, we refer to the geometry of fig. 8, assuming the numeric case of the previous example of fig. 7.

Besides, we assume the camera axis along the orthogonal direction to terrestrial magnetic field (of intensity B=0.6 Gauss) and the electrons energy at the deflection plates of 1 keV. The electron velocity along camera axis will be then $v_x=\sqrt{\frac{2eV}{m}}=1.87\text{x}10^7$ (m/s). Comparing the centripetal force to the Lorentz one, $\frac{mv_x^2}{R} = ev_xB$, the radius R of the electron results of:

$$R = \frac{v_x}{\frac{e}{m}B}$$

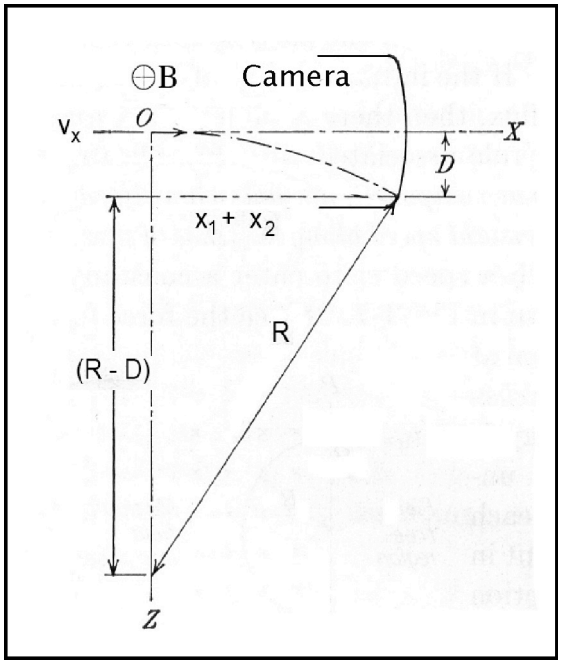


Fig. 8: D deflection of the electron path due to terrestrial magnetic field B orthogonally going into the figure.

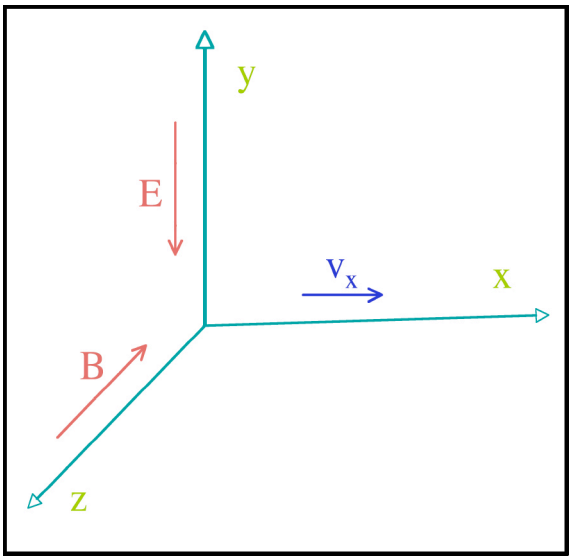


Fig. n. 9: Corrector electric field E and terrestrial magnetic field B orthogonal between them and perpendicular to the flying velocity $v_x$.

From geometry of fig. 8, the equation of the magnetic deflection is deduced:

$$R^2 = (R - D)^2 + (x_1 + x_2)^2$$

that corresponds to a value of D=36.84 mm. Of course, if the direction of motion is not perpendicular to magnetic field, electron deflection becomes smaller. In any case, this strong effect must be corrected. A way for doing this it is to screen the vacuum chamber using antimagnetic cylinders of mu-metal that will however make more difficult the access to the chamber during measurements screen the vacuum chamber. Another way, at which we think to recourse, is to use an electric corrector field. In this case, with reference to the fig. 9, we get

$$v_x = \frac{E}{B} = u$$

Therefore, with our assumption:

E=1122 volts/m

Which corresponds to a voltage of 41.33 V.

### 2.1.5 MCP and multi-anodic system

Forward to the flight cell, a micro-channel plate (MCP) detector is placed. Between the two MCP configurations, J shaped single stage or Chevron double stages, we selected the former for the final target of the camera, because it assures a gain high enough of electrons and a best reduction of the electronic cloud size.

However, in the prototype phase the Chevron configuration will also be useful, because, apart from assuring a good gain of electronic intensity (at lower tension of power supply), it will allow to maintain a good reduction of the electronic cloud size passing through from 1^ to 2^ stage (see fig. 10; Chevron double stage: thickness D=0.41 microns per single stage; channel diameter=10 microns; channel pitch=12 microns; bias angle=8.13 degrees; effective diameter=27 mm).

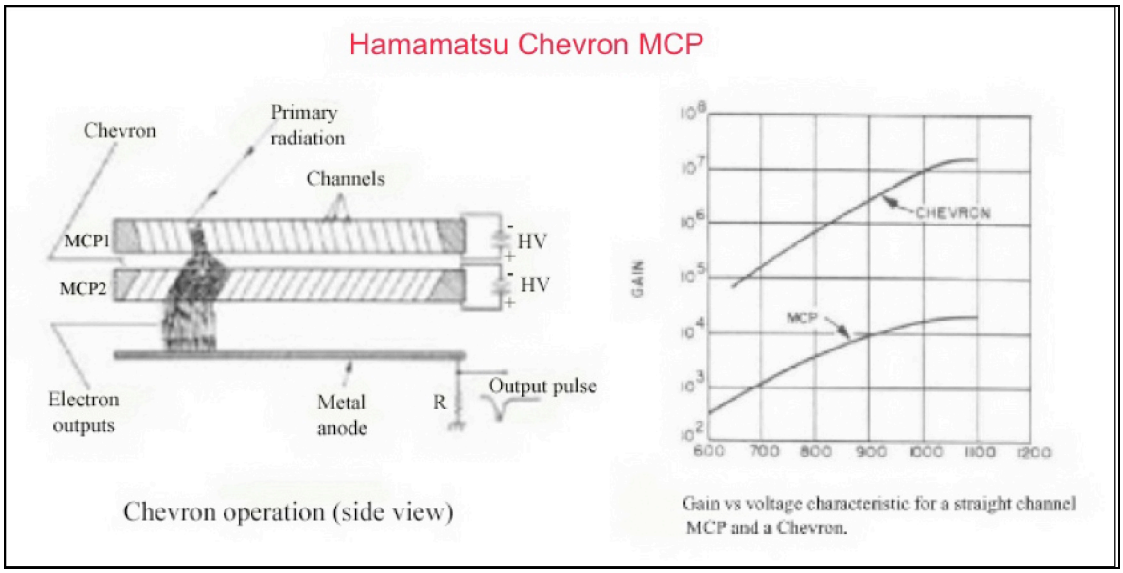


Fig. 10: MCP Chevron configuration (credit to Hamamatsu).

The charge coming out of the MCP channels is not sent onto a phosphor surface as it is usually made. This is because the light due to the electron beam conversion suffers for multiple scattering by phosphor grains and the signal profile results more large than that detected for direct conversion of the electron beam, as it is schematically shown in fig. 11 (a) and (b). The scattering causes image blur and resolution loss.

The our charge, coming out of the MCP channels, is instead collected by a multi-anode system xy, customized to aim for mapping directly the phenomenon temporal sampling. In our case, the area, used by MCP, will be subdivided in 1280 ‘pads’, arranged in 128 time channels for 10 wavelength intervals, for which each ‘pad’ will have a size less than 2 $mm^2$ (see you fig: 12).

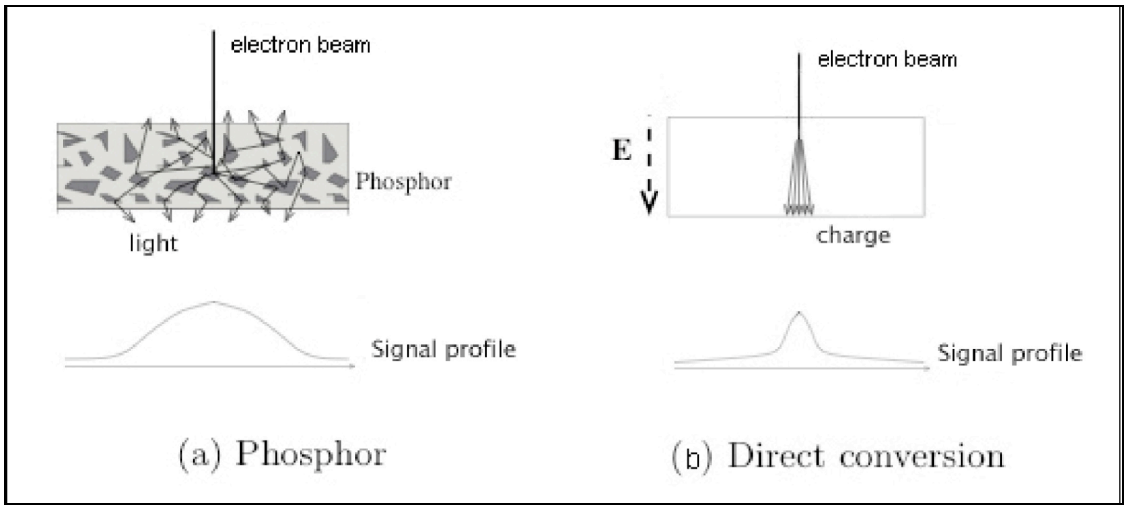


Fig. 11: Charge detecting: a) by phosphor with light production suffering for multiple scattering and b) by direct conversion.

The multi-anode layout can be read with accuracy better than 10 ps on the variation of the electronic path. It is possible to arrange a finer time read system disposing all the 1280 pads distributed in 1280 channels for only one wavelength. In this case it is possible to get to 1 ps of accuracy on the electronic path variation.

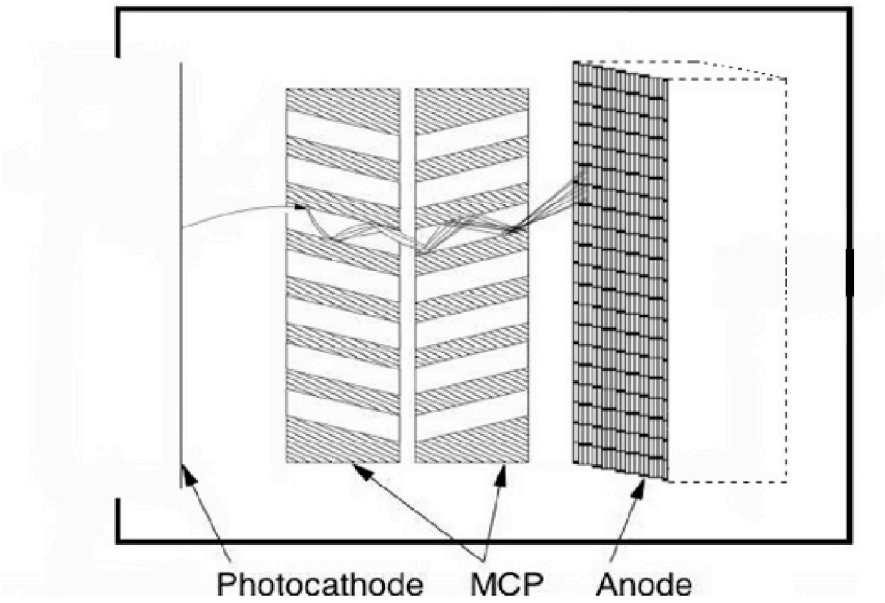


Fig. 12: Multi-anode system XY.

To obtain the best time resolution we will use a MCP (Hamamatsu or BURLE) with a C-to-C pitch of 6-12 microns, that, with the used spatial geometry (geometric magnification 10-100) at least in theoretical line allows to maintain a resolution of 6÷12 parts on about 20000. The electron transit time jitter into MCP cannot influence time resolution, being temporal distribution directly converted in spatial dimension. Vacuum of order of $10^{-6}$ mbar, gotten in the vacuum chamber with dry mechanical and turbo-molecular pumps and gages controls, assures MCP good operation.

## 3. Electronic system

The detector electronic system is shown in block-diagram of fig. 13.

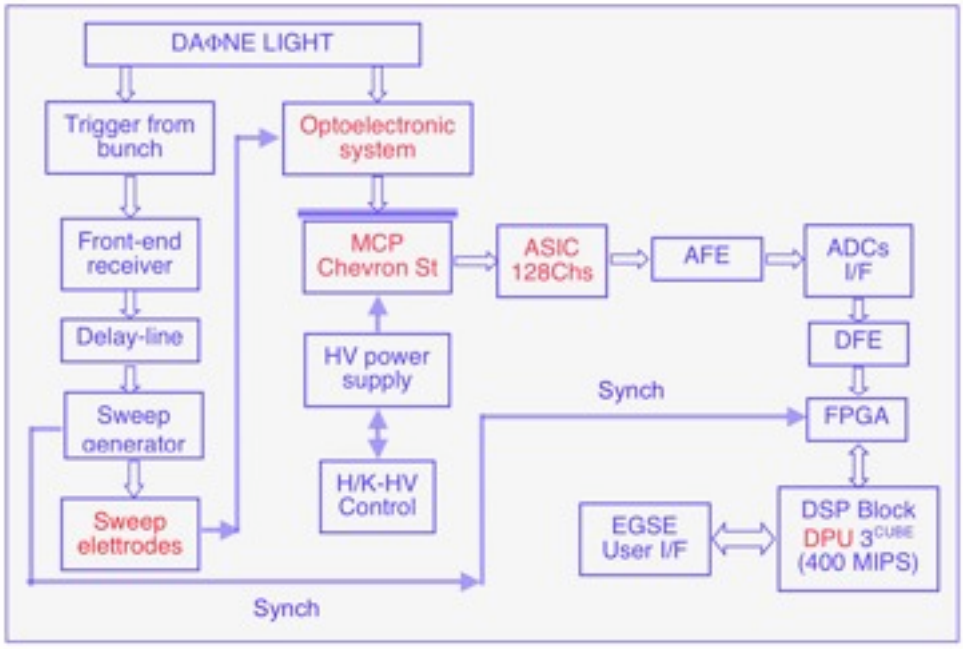


Fig. 13: Electronic block-scheme with synchronization from machine trigger bunch.

It is constituted from: 1) trigger system chain of the machine bunches which synchronizes 'Sweep generator' to streak ‘Sweep electrodes', 2) MCP high voltage power supply and control and 3) analogical/digital electronics collecting and processing charge signals coming from MCP pads.

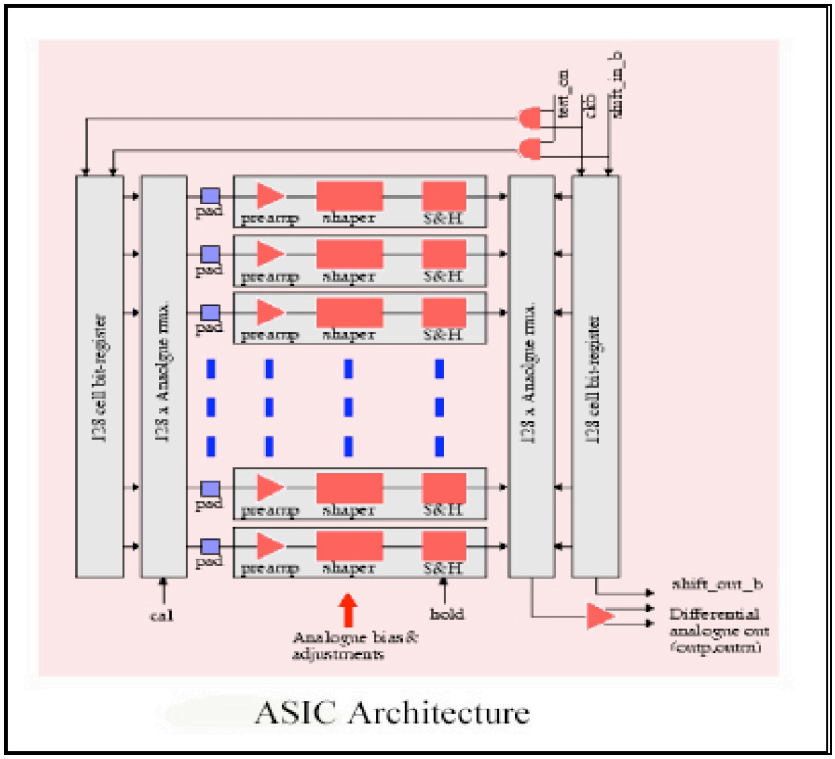


Fig. 14: Identical 128 parallel sensitive charge amplifiers [from Ideas ASA specifications 2006, Norway].

Regarding high voltage we think to put in a system, locally integrated, a HV power supply miniaturized micro-module of volume 1 $cm^3$, directly controlled in voltage and remotely connected from a little I/F, operating at low level of voltage [5].

The collecting charge signal electronics will use commercial ASIC, constituted by chip of identical 128 parallel sensitive charge amplifiers, see you fig. 14 (ASIC parameters: Process: 0.8 micron N-well CMOS; Size: 6.12 mmx4.04mm, thickness: ~600 μm; Radiation hardness: 1 Mrad; Max read-out 10 MHz).

The data handling system is based on a digital processing unit $3^{Cube}$ DSP, originally developed for space applications [6]. This unit is particularly suitable for its high performances to the front-end local processing (3Cube MINI-DPU block properties: 400 MIPS/200 MHz; 4 Meg x 16 DRAM; 1 Meg x 16 Flash Memory; 192 Kilobyte SRAM access memory time less than 5nsec; 32 Kilobyte SPI Flash Memory; 3 x 100Mbit/s bidirectional serial buses; 4x10 bit ADC channels). This resource is integrable with controllers based on FPGA, fig. 15, which can drive systems until to 6 inputs of multi-anode detectors, each ones whose is equipped with correlated double sampling I/F, gain and offset compensation. These controllers, interfaceable with PC host by USB 2.0 (480 Mb/sec), suitably adapted, can be integrated to the local calculation resources of $3^{Cube}$ DPU (controller properties: 6 x 14 bit independent analogical channels with sample rate of 15 MHz or 6x8 bit with 30 MHZ of sample rate; USB 2.0 PC Host I/F, 480 Mb/sec; FIFO buffering of 264 Kbytes). It is, however, under consideration a direct data transfer on bus PC of type PCI Express 16x of an optical system based on sensor CMOS (in this application eventually usable like optical monitor) at high read-out rate (4000 FPS, frame of 1280x128 pixels, with extension to 1280x 1024 pixels).

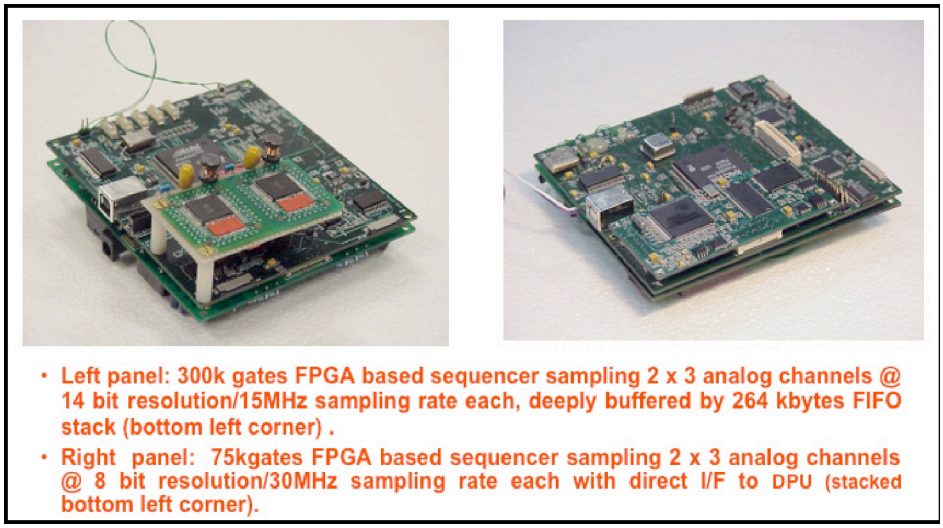


Fig.15: FPGA controllers at 14 bits of resolution and 15Mhz and at 8 bits and 30 MHz (by AMDL).

Preliminary tests of photoelectron optical alignment will be done during the experiment by coupling to MCP a system based on ‘wedge and anodes’ (WSA), whose our group is already in possession. In this configuration the coordinates X,Y of the impact electron can be process to a rate of 1 MHz with a typical space resolution of 512x512 pixels. The centroid position X,Y is determined by the charge signal ratio of the three anodes Qs Qw Qz on which the charge of MCP has been divided for induction (anode pitch 0.5 mm, resolution 20 microns). The WSA read-out will be strongly eased by availability of the FPGA controllers at 6 channels previously described.

**4. Mechanical apparatus**

In fig. 16 we report a perspective view, scheming FASTEST-CAM inside. The vacuum chamber is constituted by a cylindrical tube of length 500 mm and diameter 160 mm, ended by two flanges with 200 mm of diameter. In the figure, the flange of incident light, holding calcium fluorite ($CaF_2$) window, is on the top right. The exit flange is on the bottom left and has linked the barrel, housing the ASIC electronic read-out. Two small lateral flanges hold low and high electric power supplies and connectors for the radiofrequency synchronization.

Starting from the entry window on the top right the different components have been represented in following order:

1) calcium fluoride window (on red small cylindrical flange),
2) photocathode (on square blue support),
3) first three pairs of accelerator grids for electronic beam,
4) focussing electrical quadrupole (little rectangular black box),
5) second pairs of accelerator grids,
6) pair of deflection plates of the electronic beam (in light grey),
7) pair of dispersion plates of the electronic beam, orthogonal to deflection plates,
8) MCP device on cylindrical flange,
9) multianode system, ended on the exit flange,
10) electronic cards and cover barrel on the bottom left.

All these parts will be aligned and assembled on a rigid support, provided of movement to be driven from the outside for fine alignments, after that the cylinder vacuum chamber is closed.

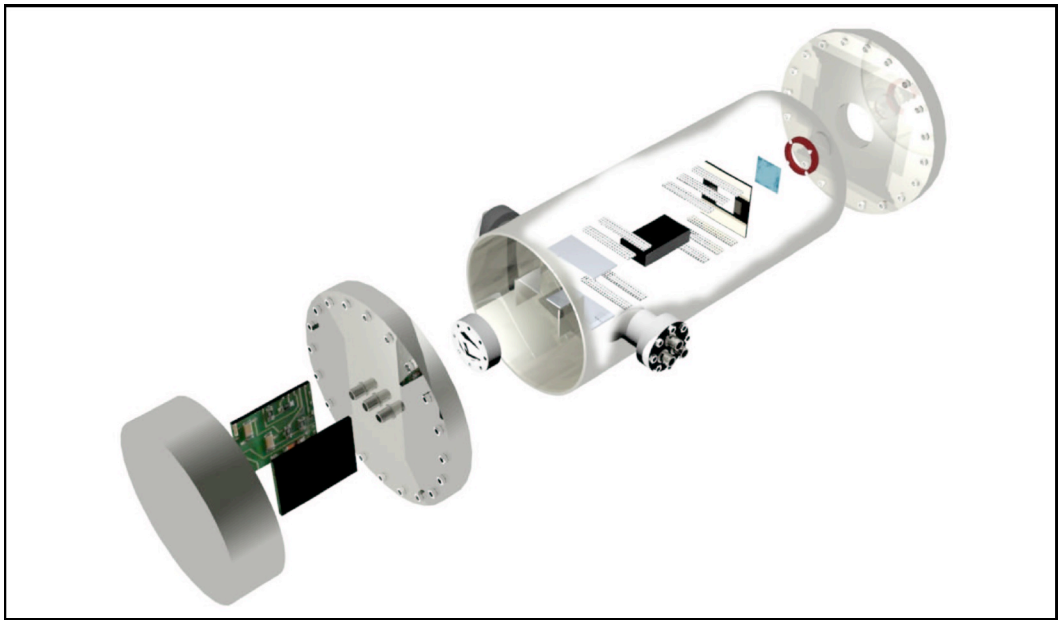

Fig. 16: Perspective view of FASTEST-CAM inside.

**4. Developing project plan**

FASTEST-CAM will be developed in two years for a total cost of ~110 kE. It is necessary to have support of 1 month of man power per year from Mechanical Design Service and from

Electronic Service of LNF-INFN, respectively, for the relative designs, assemblies, electronic wiring up and support to laboratory tests. It is request 1 mouth for year of DAΦNE machine time shifts in each of two years, respectively.

In the first year, the required machine shifts consist for using in an experimental hall a machine radiofrequency trigger, suitable to synchronize the deflecting plate electronics of the electron beam of FASTEST-CAM. In such a case we observe we can operate in parasitic mode without interfering at all with other users who have dedicated the machine time shifts. A pair of dedicated time machine shifts will be however necessary at the end of the first year to verify the photocathode spectral response to the synchrotron radiation in the band utilized by the experiment (photocathode previously experimented in laboratory with conventional sources) and to do a final test of synchronism with the light. On the second year, the machine time shifts instead will serve for characterizing the whole instrument, for doing the proposal fluorescence measurements with synchrotron radiation bunches, for effecting the first tests of diagnostic and visualization of the time and space fluctuations of the machine light pulses.

With this aim we report in fig. 17 the expressive images of the machine bunches done some years ago at ESRF and LEP with a standard streak-camera operating at about some hundred of Hz of frequency, showing bunch vertical movement (head-tail) instability and bunch longitudinal length fluctuations [7].

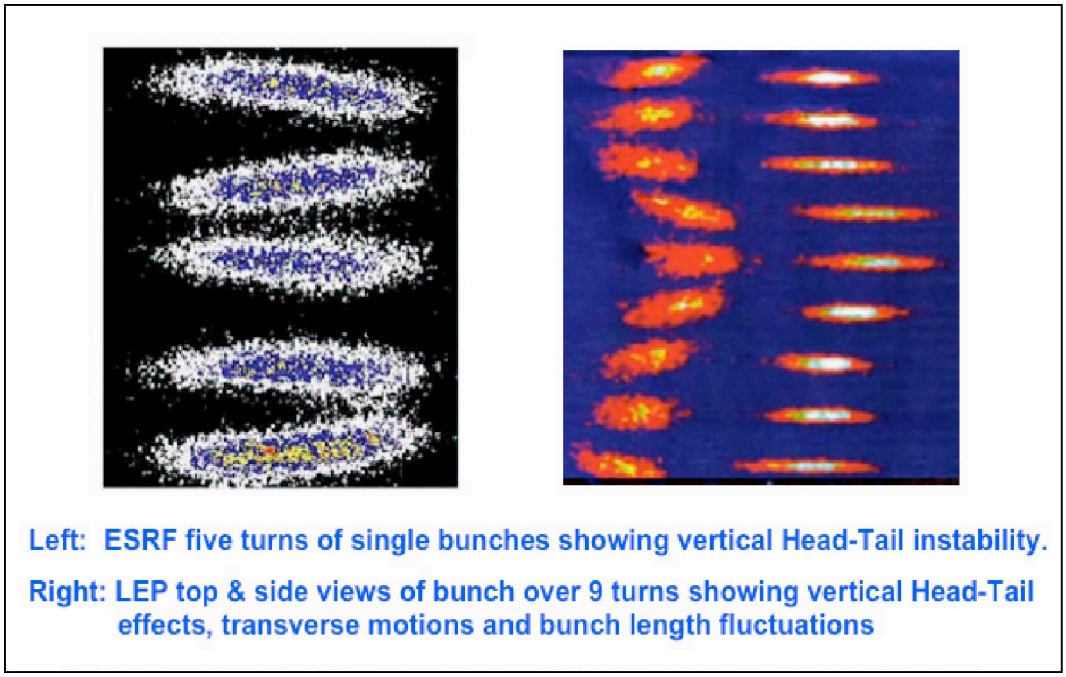


Fig. 17: Bunch vertical movement (head-tail) instability and bunch longitudinal length fluctuations [pictures from ref. 7].

**7. Conclusions**

In conclusion, the proposed FASTEST-CAM is an innovative and versatile instrumentation suitable to detect light phenomena so ultra-fast as in one picosecond [8]. Its general characteristics can be synthesized as in the following.

1. It makes simultaneous measurements of time decays and wavelengths or of space distributions of light intensity.
2. Each measurement is triggered in time synchronism by bunches of DAΦNE synchrotron source.
3. Its measurement range is 500ps-3nsec.

4. Its time resolution has been valued better than 5 ps and for the fastest sweep range down to less than 1 ps.
5. It does not use phosphor for detecting electrons, for which there are not image blur or resolution loss.
6. It makes single electron count measurements with better accuracy than those devices which at end have to reconvert electrons in light (e.g. CCDs).
7. It uses a very high integrated technology for front-end electronic (HV power supplies, ASIC, ADC, TDC), and a high powerful calculation system for signal processing and data presentation (DFE, FPGA, DPU).
8. Its count rate is estimated in 100 kHz (using the project identified ASICs) or also better.
9. It can be used, by changing photocathode, on whole synchrotron radiation spectral range from infrared to X-rays.
10. It can be use for diagnosing bunch transversal instabilities and bunch longitudinal length fluctuations of the machine.
11. It can be use for visualizing and characterizing the space-time structure of light pulses of the new FEL sources [9], in development at our LNF.

**Acknowledgements**

The authors would like to thank Mr. Bruno Ortenzi for his drawing support.

**References**

[1] C. D. McGuinness et al., A new sub-nanosecond LED at 280 nm: application to protein fluorescence, Meas. Sci. Technol. 15(2004)L1.

[2] B. Salvato et al., Saccharose solid matrix embedded protein: a new method for sample preparation for X-ray absorption spectroscopy. Eur. Biophys. J. 29(2000)391.

[3] M. M. Murnane et al., X ray streak camera with 2 ps response, Appl. Phys. Lett, 56-20(1990)1948.

[4] C. B. Johnson et al., Circular-scan streak tube with solid-state readout, App. Opt. 19(1980)3491.

[5] A. La Monaca, A highly integrated HV straw-tube powering system and process. electronics, Fermilab, BTeV Doc-2521-2v, 2004.

[6] A. M. Di Lellis, 3Cube MINI DPU, Selected for SERENA experiment for ESA BepiColombo Mission, 2004.

[7] K. Scheidt, Review of Streak Camera for Accelerators: features, applications and results. Proceedings of EPAC 2000, Vienna, Austria.

[8] D. A. Reis et al, Ultrafast X-ray physics, Rad. Phys. Chem. 70(2004)605.

[9] C. Vaccarezza et al., Status of the SPARX FEL Project, Presented at the 10th Particle Accelerator Conference (PAC2006), 2006 - Edinburgh, UK; LNF-06-23(P).